JOURNAL OF VIROLOGY, Sept. 1997, p. 6749–6756 Vol. 71, No. 9
0022-538X/97/$04.00+0

Functional and Structural Analysis of the Sialic Acid-Binding Domain of Rotaviruses

PAVEL IŠA,[1]* SUSANA LÓPEZ,[1] LORENZO SEGOVIA,[2] AND CARLOS F. ARIAS[1]

Departamento de Genética y Fisiología Molecular[1] and Departamento de Reconocimiento Molecular y Bioestructura,[2] Instituto de Biotecnología, Universidad Nacional Autónoma de México, Cuernavaca, Morelos 62250, Mexico

Received 19 February 1997/Accepted 28 May 1997

The infectivity of most animal rotaviruses is dependent on the interaction of the virus spike protein VP4 with a sialic acid (SA)-containing cell receptor, and the SA-binding domain of this protein has been mapped between amino acids 93 and 208 of its trypsin cleavage fragment VP8. To identify which residues in this region are essential for the SA-binding activity, we performed alanine mutagenesis of the rotavirus RRV VP8 expressed in bacteria as a fusion polypeptide with glutathione *S*-transferase. Tyrosines were primarily targeted since tyrosine has been involved in the interaction of other viral hemagglutinins with SA. Of the 15 substitutions carried out, 10 abolished the SA-dependent hemagglutination activity of the protein, as well as its ability to bind to glycophorin A in a solid-phase assay. However, only alanine substitutions for tyrosines 155 and 188 and for serine 190 did not affect the overall conformation of the protein, as judged by their interaction with a panel of conformationally sensitive neutralizing VP8 monoclonal antibodies (MAbs). These findings suggest that these three amino acids play an essential role in the SA-binding activity of the protein, presumably by interacting directly with the SA molecule. The predicted secondary structure of VP8 suggests that it is organized as 11 β-strands separated by loops; in this model, Tyr-155 maps to loop 7 while Tyr-188 and Ser-190 map to loop 9. The close proximity of these two loops is also supported by previous results from competition experiments with neutralizing MAbs directed at RRV VP8.

Rotaviruses have been identified as the single most important etiologic agent of gastroenteritis in infants and young animals worldwide (17). They are composed of a segmented double-stranded RNA genome surrounded by three concentric layers of proteins (43). The surface of rotaviruses contains two proteins, VP4 and VP7. VP4 forms the viral spikes (1, 36) and has been associated with a variety of viral functions, including cell attachment and penetration (6).

The attachment of most animal rotaviruses to epithelial cells and the ability of these viruses to agglutinate erythrocytes (hemagglutination [HA]) are mediated by sialic acid (SA)-containing compounds (10, 18, 30, 52). Treatment of cells with sialidases inhibits HA and greatly reduces the binding of virus to the host cell surface, with a consequent reduction in virus infectivity. In addition, HA and the binding to target cells can be inhibited by incubation of the virus with several sialoglycoproteins, including glycophorin A (gphA). These observations suggest that the VP4 domain which recognizes SA on the target cells is the same that binds to SA in erythrocytes. In the case of animal rotavirus infection, it has been proposed that the initial attachment to SA is followed by a second interaction of the virus particle with an SA-independent molecule, which has not been identified so far (30). In contrast to animal rotaviruses, the rotavirus strains isolated from humans do not hemagglutinate, and their infectivity does not depend on SA and is not inhibited by gphA (10, 30).

The use of SA by rotaviruses as their cellular receptor is not unique among viruses. SA has been described to be, or form part of, the receptor for many viruses, including various coronaviruses (48), influenza virus (49), reovirus type 3 (35), murine polyomavirus (45), and Sendai virus (29). The best-characterized viral SA-binding domains are those of influenza virus and murine polyomavirus, whose structures complexed with SA have been resolved by X-ray crystallography (45, 49). Topographically, the SA-binding site of both influenza virus and polyomavirus is a shallow depression located on the tip of the SA-binding protein. In the influenza virus hemagglutinin, six amino acid residues (Tyr-98, Gly-135, Ser-136, Asn-137, Glu-190, and Ser-228) form hydrogen bonds with SA (41, 49). In murine polyomavirus, four amino acid residues of VP1 were proposed to interact with the receptor analog 3′-sialyl lactose; Tyr-72 and His-298 formed hydrogen bonds and Arg-77 formed a salt bridge with the SA moiety of the molecule, while Asn-93 was hydrogen bonded to galactose (45). Although there is no homology between the influenza virus and murine polyomavirus SA-binding domains, the numbers of hydrogen bonds involved in the two interactions are comparable. In these interactions, van der Waals and hydrophobic bonds might also be important (45, 49).

In animal rotavirus strains, VP4 has been identified as the virus hemagglutinin, and it has been shown that this protein does not require other rotavirus proteins to hemagglutinate (26). Expression of truncated versions of VP4 in bacteria and insect cells has shown that the HA domain lies in VP8, the smaller trypsin cleavage polypeptide of VP4 (8, 21). Recently, through the expression in insect cells of chimerical VP4 proteins, it was shown that the region between VP4 amino acids 93 to 208 of the porcine rotavirus strain YM is sufficient to determine the HA activity of the protein (9).

This paper reports the use of site-directed mutagenesis to investigate the involvement of selected amino acids in the binding of rotavirus RRV VP8 to SA. The results are presented in the context of the prediction of the VP8 secondary structure.

* Corresponding author. Mailing address: Departamento de Genética y Fisiología Molecular, Instituto de Biotecnología, Universidad Nacional Autónoma de México, Apartado Postal 510-3, Cuernavaca, Morelos 62250, México. Phone: (52) (5) 6227612. Fax: (52) (73) 172388. E-mail: pavel@ibt.unam.mx.

MATERIALS AND METHODS

Cloning of VP8 and site-directed mutagenesis. The parental RRV, YM, and Wa VP8 genes (VP4 gene nucleotides 1 to 750) were cloned in pGEX-4T-1 (Pharmacia) essentially as previously described (22). Briefly, partial-length double-stranded cDNA of the VP4 genes was produced by PCR amplification with oligonucleotides complementary to conserved VP4 gene nucleotides 1 to 18 (oligonucleotide 5′) and 731 to 750 (oligonucleotide 3′). The oligonucleotides had additional recognition sequences for the restriction endonucleases *Bam*HI (5′ oligonucleotide) and *Eco*RI (3′ oligonucleotide) at their 5′ ends, which were used to clone the amplified DNA into the *Bam*HI and *Eco*RI sites of plasmid pGEX-4T-1 (Pharmacia). Two stop codons were included in the 3′-specific oligonucleotide following the codon AGA for arginine 247, to ensure termination of translation. The fusion protein GST-VP8 contained 226 amino acids from the glutathione *S*-transferase (GST) protein and the thrombin cleavage site, 3 amino acids resulting from translation of the 9-nucleotide 5′-noncoding region of rotavirus gene 4, and 247 amino acids (246 for Wa) of VP8, resulting in a fusion protein of approximately 58 kDa. Alanine-scanning mutagenesis of RRV VP8 was done by megaprimer PCR, as described by Merino et al. (32), adapted for the pGEX vector. Three primers (A to C) were designed to be used for mutagenesis of any fragment inserted into pGEX vectors. Primers A (5′ GGAATAGCCGATCGAGATCCGGGAGCTGCATGTGTCAGAGG 3′) and C (5′ GGGCTGGCAAGCCACGTTTGGTG 3′) have sequences complementary to pGEX (underlined), while primer B (5′ GGAATAGCCGATCGAG ATCCGGG 3′) is not complementary to pGEX and therefore should amplify only the DNA extended from primer A. A 100-μl PCR mixture was used with 1 ng of pGEX-4T-1/RRV VP8 combined with 50 pmol each of primer A and a second primer designed to introduce the desired mutation. This mixture was then subjected to 30 cycles of reaction under the following conditions: 1 min at 94°C, 2 min at 42°C, and 3 min at 72°C (reaction 1). The product of reaction 1 was gel purified, and 10 μg was used as the megaprimer with 10 μg of template (pGEX-4T-1/RRV VP8 linearized with *Eco*RV) in a 90-μl reaction mixture for five cycles of 1 min at 94°C, 2 min at 50°C, and 2 min at 72°C (reaction 2). The resulting extension product was amplified by adding 50 pmol each of primers B and C, bringing the total volume to 100 μl, and performing 30 additional cycles (reaction 3). The product of reaction 3 was digested with *Bam*HI and *Eco*RI to generate the mutagenized 750-nucleotide RRV VP8 gene, gel purified, and cloned into pGEX-4T-1 prepared accordingly. To help in the detection of mutants, specific restriction enzyme sites were introduced and/or knocked out without affecting amino acid codons, unless an amino acid change was desired. The VP8 genes of YM and Wa were mutagenized essentially as described by López et al. (23). The presence of the desired mutations was confirmed by sequencing with Sequenase 2.0 (United States Biochemicals) as specified by the manufacturer.

Expression and purification of recombinant VP8 proteins. For expression of the rotavirus parental and mutated VP8 proteins in *Escherichia coli* JM109, Luria-Bertani medium (containing 100 μg of ampicillin per ml) was inoculated with a 1:10 dilution of an overnight culture and the bacteria were grown for 3 h at 28°C and induced for 2 h at 28°C with isopropyl-β-D-thiogalactopyranoside (IPTG) at a final concentration of 0.75 mM. Cells from 20-ml cultures were collected by low-speed centrifugation (5,000 × *g*) and resuspended in 1 ml of 0.2 M NaCl–2.7 mM KCl–1.4 mM KH_2PO_4–0.8 mM Na_2HPO_4, and the protease inhibitor phenylmethylsulfonyl fluoride was added to a final concentration of 1 μM. The bacteria were disrupted by sonication and then incubated at room temperature (RT) for 15 min with 0.5% Triton X-100. The insoluble fraction was separated from the supernatant by centrifugation at 8,300 × *g*, and the supernatants were used in the subsequent assays. If desired, proteins were purified from supernatants with glutathione-agarose beads (Sigma Chemical Co.) as described previously (42).

Quantitation of proteins. The fusion proteins were quantified by Western blot analysis. The proteins in the sonicate supernatants were separated by sodium dodecyl sulfate-polyacrylamide gel electrophoresis (SDS-PAGE), with 11% running and 4% stacking gels, by the method of Laemmli (19). After SDS-PAGE, the proteins were electrophoretically transferred to nitrocellulose (Schleicher & Schuell) with the SemiPhor system (Hoefer). The membranes were washed quickly in deionized water and blocked for 1 h at RT with phosphate-buffered saline (PBS)–5% (wt/vol) nonfat dry milk. The membranes were rinsed twice in PBS–0.1% milk (washing buffer) and incubated for a minimum of 2 h at RT with hyperimmune rabbit anti-rotavirus YM antiserum (YM neutralization titer, 1:100,000) diluted 1:5,000 in washing buffer. Unbound antibodies were removed with three exchanges of washing buffer, and after the addition of affinity-purified peroxidase-labeled goat anti-rabbit immunoglobulin G (IgG) antibody (0.2 mg/ml) (Kirkegaard & Perry) diluted 1:2,000 in PBS–0.1% milk, the incubation proceeded for a minimum of 2 h at RT. After the membrane was washed as described above, the specific protein was detected by enhanced chemiluminescence (ECL; Amersham) and its relative amount was determined with wild-type GST-VP8 as the standard. Alternatively, following purification with glutathione-agarose beads, the proteins were quantified by the DC protein assay (Bio-Rad) with bovine serum albumin (BSA) as a standard.

HA. Serial twofold dilutions of bacterial supernatants or purified proteins in PBS–0.125% BSA were made in 96-well V-shaped vinyl plates (Costar). To 50 μl of these dilutions, 50 μl of 0.4% human type O erythrocytes in PBS–0.125% BSA was added, and the plates were left at RT for 1 h before the titers were recorded.

Antigen capture ELISA. The binding of monoclonal antibodies (MAbs) to the *E. coli*-produced GST-VP8 proteins was assessed by an antigen capture enzyme-linked immunosorbent assay (ELISA). Briefly, 96-well plates (Costar) were coated with a 1:1,000 dilution in PBS of MAbs M11, 1A9, M14, and 7A12 (specific for the VP8 domain of RRV VP4) (27) and incubated overnight at 4°C. Anti-VP6 MAb 255 was used as a negative control. The MAbs were kindly provided by H. B. Greenberg (Stanford University). After being coated, the plates were washed four times with PBS and blocked with PBS–1% BSA overnight at 4°C. After the washing step, equal amounts of the mutant and parental VP8 proteins (as determined by Western blot analysis) were added and the plates were incubated for 1 h at 37°C or overnight at 4°C. This was followed by the addition of hyperimmune rabbit anti-rotavirus YM antibody diluted 1:1,300, and the mixture was incubated for 1 h at 37°C. After further washings, affinity-purified alkaline phosphatase-labeled goat anti-rabbit IgG antibody (0.2 mg/ml; Kirkegaard & Perry) diluted 1:1,000 was added, and the plates were incubated for 1 h at 37°C. Finally, Sigma 104 phosphatase substrate in diethanolamine buffer (pH 9.8) was added, and after 1 h of incubation at 37°C, the optical density at 405 nm (OD_{405}) of the wells was determined. The cutoff was set at an OD_{405} of 0.2.

The mutant proteins were arbitrarily considered to have a severely distorted structure if their reactivity with two or more MAbs was less than 50% of that of parental GST-VP8. The proteins that reacted with at least three MAbs at levels between 50 to 75% of those of GST-VP8 were considered to have a mildly distorted structure. A mutant protein with a reactivity of more than 75% of that of GST-VP8 for all four MAbs tested was considered to have an unaffected structure.

Binding of recombinant rotavirus VP8 to glycophorin A. Plates (96 wells; Costar) were coated with 31 ng of gphA (Sigma Chemical Co.) per well in PBS. After overnight incubation at 4°C, the plates were washed four times with PBS and blocked with PBS–1% BSA, as described above. The same amount of protein as used in the ELISA was added, and the plates were incubated overnight at 4°C. The protein bound to gphA was detected with the hyperimmune rabbit anti-rotavirus YM antibody, as described above.

Secondary-structure prediction. The secondary structures of six individual VP8 sequences (strains RRV [GenBank accession no. M18736], L338 [L26888], KU [M21014], K8 [D90260], YM [M63231], and B223 [M92986]), which represent different branches of a VP4 phylogenetic tree (47), were predicted by a self-optimized prediction method (SOPM) (12). This method, available from http://www.ibcp.fr/predict.html, uses five different algorithms: the Gibrath method, the Levin method, the DPM method, SOPMA, and PHD. A final consensus for each rotavirus strain was used for the comparison shown in Fig. 2. The secondary-structure probability and tertiary class of these six VP8 proteins were also computed by using the protein structure analysis server (46, 50) available from http://bmerc-www.bu.edu/psa/request.html. Predictions of secondary structure and solvent accessibility were also obtained by comparing 57 rotavirus VP8 proteins (human isolates RV-5 [M32559], 1076 [M88480], Wa [M96825], KU, K8, 69M [M60600], Mc35 [D14032], HCR3 [L19712], Ro1845 [D14726], PA169 [L20874], 116E [L07934], HAL1166 [L20875], L26 [M58292], ST3 [L33895], AU1 [D10970], CJN [D16353], I321 [L07657], E1B [U07753], F45 [U30716], and RV3 [U16299]; simian isolates SA11 [X14204] and RRV; porcine isolates OSU [X13190], Gottfried [M33516], YM, BEN 307 [L07885], BMI-1 [L07887], CRW-8 [L07888], TFR-41 [L07889], MDR-13 [L07886], PRV 4F [L10359], and PRV 4S [L10358]; bovine isolates C486 [Y00127], UK [M22306], B223, B641 [M63267], KK3 [D14367], 61A [D13396], A44 [D13392], A5 [D13395], K33 [D13393], and 993/83 [D16352]; murine isolates Eb [L18992], EHP [U08424], EC [U08421], EL [U08426], and EW [U08429]; feline isolates FRV64 [D14723], FRV1 [D10971], Cat2 [D13403], and Cat97 [D13402]; canine isolates K9 [D14725], and CU1 [L20876]; lamb isolate Lp 14 [L11599]; and equine isolates H2 [L04638], H1 [D16341], FI14 [D13398], FI23 [D16342] and L338) by profile-fed neural network systems from Heidelberg (PHD) (http://www.embl-heidelberg.de/predictprotein/phd_pred.html) (38, 39). The parsing predictions were done by computational biochemistry, AllAll server, available from http://cbrg.inf.ethz.ch/AllAll.html, with the RRV, L338, B223, KU, K8 and YM sequences.

RESULTS

Synthesis and HA activity of rotavirus RRV VP8. The VP8-encoding region from the VP4 gene of the rotavirus strain RRV that is currently being used in our laboratory was cloned and sequenced. Comparison with the previously published (27) RRV sequence showed 13 nucleotide differences, which resulted in two amino acid changes (threonine instead of serine at position 73 and asparagine instead of tyrosine at position 132). The RRV VP8 gene was expressed in *E. coli* fused to the gene encoding GST, and it directed the synthesis of a hybrid protein (GST-VP8) of 58 kDa.

The recombinant polypeptide was synthesized in bacteria in a soluble form, being present in the supernatant of bacterial

sonicates with an HA activity that reached titers of up to 1:260,000. The GST-VP8 protein was purified from bacterial supernatants with glutathione-agarose beads. One HA unit was achieved with 5 ng of the purified polypeptide. The HA activity of GST-VP8 was inhibited by incubation of the protein with either gphA (200 ng/ml), hyperimmune anti-RRV serum (inhibition titer, 1:800), or VP8-specific MAbs M11 (titer, 1:800) and 1A9 (titer, 1:6,400). This activity was not inhibited by incubation with MAbs 2G4 and M7, directed at the VP5 trypsin cleavage product of VP4. These results indicate that the HA activity of GST-VP8 is specific. The recombinant polypeptide was also able to efficiently bind to gphA in a solid-phase assay (see below), supporting the conclusion that the SA-binding domain in the fusion protein is correctly folded. The HA-specific activity of crude bacterial supernatants containing GST-VP8 was the same as that of the affinity-purified protein; therefore, crude supernatants were used throughout this study unless otherwise indicated.

Alanine mutagenesis of RRV GST-VP8. Since the *E. coli*-produced RRV VP8 protein contained a functional HA domain, we used it as a system to map, by site-directed mutagenesis, the amino acid residues essential for the SA-binding activity of the protein. The amino acids to be mutagenized were selected based on the information available for other SA-binding viral proteins whose three-dimensional structure complexed with SA is known. Among other amino acids, tyrosine was found to form hydrogen bonds with SA in the influenza virus and murine polyomavirus hemagglutinins (45, 49). Tyrosine was also predicted to be involved in the reovirus type 3 hemagglutinin-SA receptor interaction (51). Therefore, in this work we evaluated the role of the tyrosines present in the RRV VP8 region between amino acids 93 and 208, which has been proposed to contain the HA domain of the virus (9). Ten tyrosine residues located at amino acids 119, 152, 155, 165, 175, 177, 188, 189, 194, and 206 were individually replaced by alanine residues. Tyrosine 219, which lies close to the HA domain, was also mutated. Additionally, serines 114 and 190 and asparagine 132 were changed, and one triple mutant (YYS 188–190) was constructed. Alanine was chosen as the replacement residue because it eliminates the side chain beyond the beta carbon yet does not alter the main chain conformation or impose extreme electrostatic or steric effects. Furthermore, alanine is the most abundant amino acid and is found frequently in both buried and exposed positions and in a variety of secondary structures (37).

The 14 single and 1 triple mutant genes were expressed in *E. coli* and assayed in HA and gphA-binding assays as described in Materials and Methods. The potential conformational changes induced in GST-VP8 by the mutations were evaluated by probing the structure of the proteins in an ELISA with a panel of anti-RRV neutralizing MAbs (M11, 1A9, M14, and 7A12) that have been shown to recognize conformational epitopes in the VP8 domain of VP4 (27, 28). The amino acid changes that allow RRV to escape neutralization by these MAbs have been mapped to amino acid residues 87 (Thr to Ala, MAb M11), 100 (Asp to Asn, MAb 1A9), 148 (Gln to Arg, MAb M14), and 188 (Tyr to Phe, MAb 7A12).

Four of the mutant proteins (Y119, N132, Y152, and Y206) were consistently found in small amounts in the supernatant of bacterial sonicates, with the majority of the protein being present in the insoluble fraction. These mutants showed no HA or gphA-binding activities and reacted poorly (less than 50% of the reactivity of the parental GST-VP8) with three or four of the VP8 MAbs (Fig. 1; Table 1); these results suggest that the structure of these proteins was severely distorted. The remaining 11 mutant proteins (S114, Y155, Y165, Y175, Y177, Y188, YYS188–190, Y189, S190, Y194, and Y219) were present in the supernatant in amounts comparable to those of parental GST-VP8. Three of these mutants (S114, Y194, and Y219) showed HA and gphA- and MAb-binding activities comparable to those of parental GST-VP8 (Fig. 1; Table 1), suggesting that the mutated amino acids are not involved in the interaction with SA. Mutation of Y165 resulted in 30 and 35% HA and gphA-binding activity, respectively, while mutant Y177 hemagglutinated to a level of about 1 to 2% of parental GST-VP8, without showing any detectable gphA-binding activity (Table 1). The reactivity of mutant Y165 with the VP8 MAbs was somewhat affected (Fig. 1), suggesting that its structure was mildly distorted. On the other hand, the reactivity of protein Y177 with the MAbs was severely impaired, with the exception of MAb 7A12 (Fig. 1). The remaining soluble mutant proteins (Y155, Y175, Y188, Y189, S190, and YYS188–190) did not possess HA or gphA-binding activity (Table 1). Of these, mutants Y175, Y189, and YYS188–190 presented an altered reactivity with the VP8 MAbs, suggesting a mild distortion of their structure (Fig. 1), while mutants Y155, Y188, and S190 reacted with the MAbs to levels similar to those of parental GST-VP8 (Fig. 1). The good interaction of mutants Y155, Y188, and S190 with the MAbs and their lack of HA and gphA-binding activities indicate that Tyr-155, Tyr-188, and Ser-190 are essential for the SA-binding activity of RRV VP8.

The large number of mutant proteins with a complete or partial distorted structure (9 of 15 mutants [Table 1]), as judged by their reactivity with the anti-RRV VP8 MAbs, was not expected, especially since alanine mutagenesis is an accurate method for determining functional residues of proteins (5, 14). To try to understand these findings, the secondary structures of the VP8 polypeptides of various group A rotavirus strains, including RRV, were predicted and analyzed.

Secondary-structure prediction of rotavirus VP8. The secondary structures of six individual rotavirus VP8s were predicted by the SOPM and PSA methods (see Materials and Methods). These two methods differ substantially, as SOPM is based on amino acid propensities whereas the PSA method is based on hidden Markov models (HMM) generated on each class of proteins. The six rotavirus VP8s were also used for parsing predictions, which identify regions where secondary-structure elements (α helix or β strand) break because of the presence of certain amino acids (for example, proline or glycine) or because of insertions (or deletions) in the compared sequences. Since multiple-alignment-based predictions are substantially more accurate than single-sequence-based predictions (40), the secondary structure was also obtained through comparison of 57 group A rotavirus VP8 proteins by PHD.

Although the VP8 proteins compared share as little as 39% amino acid identity (between strains KU and B223), there is an overall common pattern in the secondary structure present in individual- and multiple-alignment predictions. As previously observed (24), the VP8 domain of VP4 was rich in β strands. In this analysis, we refined that observation and found the presence of 11 β strands by PHD; these strands were also present in individual VP8s (Fig. 2), with the exception of β strand 8, where most individual predictions suggest an α helix. The β strands are predicted to be separated by loops, which is also supported by strong parsing predictions (Fig. 2). Flanking the β strands are two small α helices predicted by the PHD method, with the first also being present in individual predictions (Fig. 2). The PSA method predicted essentially the same secondary structure as that obtained by the SOPM method (data not shown). The major folding class of the six VP8 proteins analyzed was determined on the PSA server as diffuse

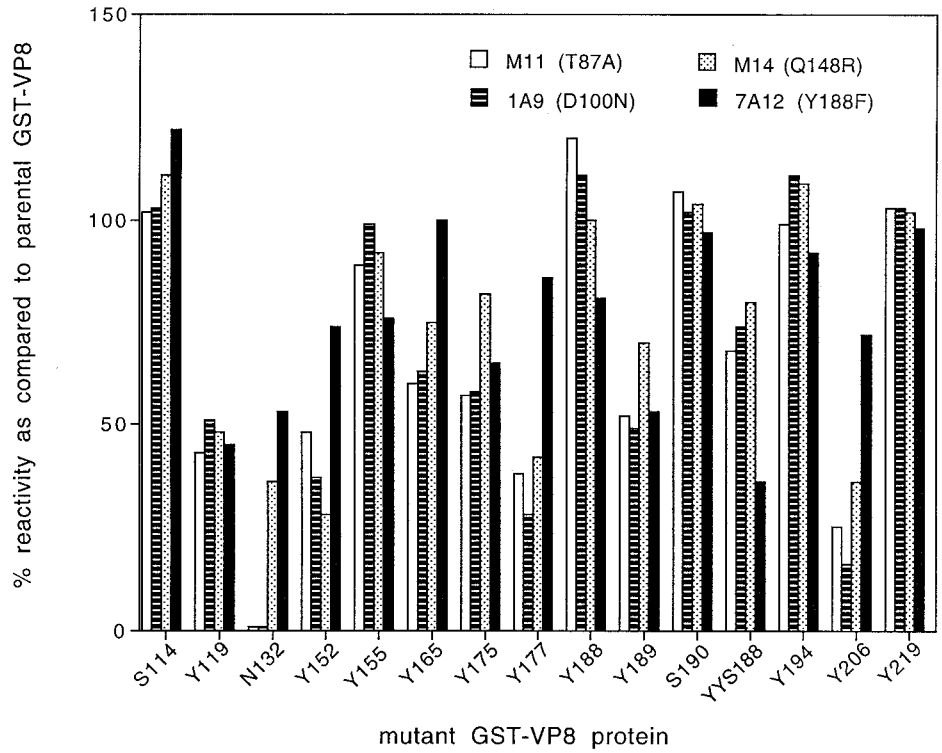

FIG. 1. Structural analysis of the GST-VP8 mutant proteins. The effect of mutations on the structure of the mutagenized proteins was analyzed by ELISA with a panel of anti-VP8 neutralizing MAbs. Equivalent amounts of the mutant proteins, compared to parental GST-VP8, were used in all experiments. The results are expressed as the mean percentage of a minimum of four independent measurements. The amino acid substitutions in the escape mutants selected with the MAbs (27) are indicated in parentheses after the MAb name. The reactivity of the MAbs with parental GST-VP8 was in the OD_{405} range from 0.45 to 1.0. The standard error of the mean was between 1 and 20% in all experiments, apart from the N132 mutant with MAb 7A12 (31.1%) and mutant Y188 with MAb 7A12 (36.8%).

beta (DB). This macroclass has a large standard deviation on both the length and number of strands, and it covers variable β domains (46, 50).

Of the residues mutagenized in this study, nine (S114, N132, Y152, Y155, Y188, Y189, S190, Y194, and Y219) were predicted to be present in coils and therefore to be part of the protein loops (Table 1). Of interest, among these amino acids were the three residues (Y155, Y188, and S190) that when mutated abolished the SA-binding activity of GST-VP8 without affecting its structure. This observation supports the idea that these amino acids are exposed on the surface of the protein and thus is consistent with their potential involvement in the binding to SA. Three other mutations located in loops (S114, Y194, and Y219) rendered proteins that reacted in all assays the same as parental GST-VP8, while the remaining mutations in coil-forming amino acids (N132, Y152, and Y189) resulted in mild or severe distortion of the protein structure. N132 is absolutely conserved among 57 group A rotavirus strains, with exception of the RRV strain reported by Mackow et al. (27), which has a tyrosine at this position. Similarly, Y189 is highly conserved among rotaviruses, with the exception of the human isolates KU, L26, RV5, E1B, CJN, Wa, 1076, and ST3 and the porcine isolates Gottfried and PRV 4F, which have a serine at this position. These amino acids, despite being in protein loops, might play an important structural role for the protein. The structural perturbation caused by the Y152 mutation is more difficult to understand, since other VP4 proteins have phenylalanine or isoleucine at this position; however, the side chains of these replacing amino acids may be capable of substituting the volume of the tyrosine phenoxyl ring, while the alanine methyl group may not.

Five other mutants (Y119, Y165, Y175, Y177, and Y206) are predicted to be part of β strands (Fig. 2), and only two of these (Y165 and Y177) bound weakly to SA. All five mutants showed distortion in their protein structure, from the severe alteration

TABLE 1. Functional and structural properties of the mutant proteins, secondary-structure prediction for the mutated amino acids, and effect of mutations on protein structure

Protein	% Activity[a]		ssp by SOPM[b]	Effect on protein structure[c]
	HA	gphA		
GST-VP8	100	100		
S114	110	117	Coil	None
Y119	0	0	β strand	Severe distortion
N132	0	0	Coil	Severe distortion
Y152	0	0	Coil	Severe distortion
Y155	0	0	Coil	None
Y165	30	35	β strand	Mild distortion
Y175	0	0	β strand	Mild distortion
Y177	1	0	β strand	Severe distortion
Y188	0	0	Coil	None
Y189	0	0	Coil	Mild distortion
S190	0	0	Coil	None
YYS188–190	0	0	Coil	Mild distortion
Y194	100	100	Coil	None
Y206	0	0	β strand	Severe distortion
Y219	110	127	Coil	None

[a] HA and gphA-binding activities are expressed as a percentage of that of parental GST-VP8, which is set to 100%.

[b] Secondary-structure prediction (ssp) for the protein region where the amino acid change is located.

[c] Effect of mutations on protein structure, as determined by reactivity with VP8-specific MAbs in an ELISA (from Fig. 1). The criteria to establish the degree of alteration of the protein structure are described in Materials and Methods.

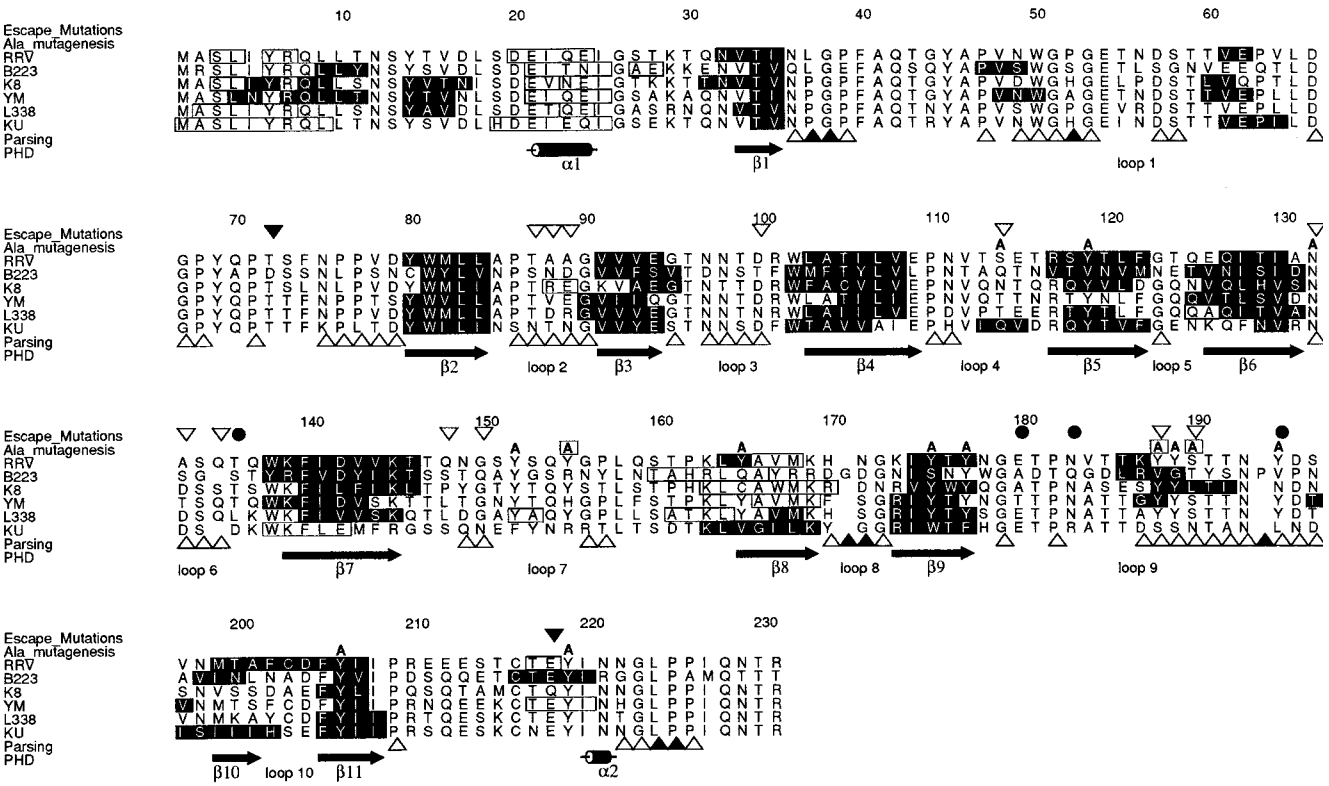

FIG. 2. Alignment of VP8 amino acid sequences. RRV, B223, K8, YM, L338, and KU deduced amino acid sequences were aligned with the program Clustalw. SOPM individual secondary-structure predictions are indicated as follows: α helices are in open boxes, and β sheets are in black. The top line indicates the location of escape mutations in the RRV (open downward triangles), ST3 (solid downward triangles), and SA11 equivalent positions (solid circles). The positions of the alanine replacements are indicated by an "**A**" on the second line. The mutations which abolished the SA-binding activity of GST-VP8 (Y155, Y188, and S190) without affecting its structure are indicated by an "**A**" enclosed in an open square. AllAll parsing predictions are indicated by upward triangles; solid triangles indicate very strong parsing predictions. The bottom line indicates the PHD prediction obtained from the 57 aligned sequences; α helices are indicated by cylinders, and β strands are indicated by arrows. Secondary-structure elements are numbered according to their position. The sequences are numbered according to the RRV sequence. Strains RRV, YM, and L338 are HA positive, and strains B223, K8, and KU are HA negative.

in mutants Y119, Y177, and Y206 to the mild perturbation in the remaining two (Fig. 1).

The intrachain RRV VP8 disulfide bond is not required for HA activity. The VP4 protein of rotavirus strains isolated from animals has five cysteines (at positions 203, 216, 318, 380, and 774) that are conserved in most strains sequenced so far. For RRV VP4, cysteines 203 and 216 and cysteines 318 and 380 are involved in forming intrachain disulfide bonds (34). In contrast, most human rotaviruses (which do not hemagglutinate) and nonhemagglutinating animal rotavirus strains lack the Cys-203 and therefore do not have a disulfide bridge in VP8.

To analyze the structural importance of the VP8 disulfide bond for the conformation of the SA-binding domain, the VP8 Cys-203 of the HA-positive porcine rotavirus strain YM was mutated to serine and the VP8 Ser-202 of the HA-negative human rotavirus strain Wa was mutated to cysteine. Both parental YM and Wa VP8 proteins and their mutants were expressed as GST fusion proteins, purified with glutathione-agarose beads, and tested in HA and gphA-binding assays. Construct YM GST-VP8/C203S reacted in both assays at levels similar to parental YM GST-VP8, while neither parental Wa nor Wa GST-VP8/S202C showed any HA or gphA-binding activity (results not shown).

DISCUSSION

The initial step in the interaction of most animal rotavirus strains with the host cell is the binding of the virus particle to a SA-containing cell receptor. This interaction is mediated by the virus spike protein VP4 and is required for the efficient attachment of the virus to susceptible cells both in vitro and in vivo (4, 10, 16, 25, 30). In this study we have characterized the SA-binding domain of rotavirus RRV by site-directed mutagenesis of the VP8 domain of VP4 expressed in bacteria as a fusion polypeptide with GST.

The *E. coli*-produced GST-VP8 fusion protein hemagglutinated to high titers; 1 HA unit was achieved with about 5 ng of the hybrid polypeptide, compared to 16 to 25 ng required for the baculovirus-expressed full-length rotavirus VP4 protein (9, 26), indicating that VP8 folds as well in bacteria as in insect cells. The HA activity of the recombinant polypeptide was present in the soluble fraction of bacterial sonicates. This activity is most probably due to multimeric forms of the hybrid polypeptide promoted by the GST component of the hybrid, since GST is known to form dimers (20).

The overall folding of 6 of the 15 mutant proteins constructed was indistinguishable from that of the parental GST-VP8, as determined by their reactivity with different conformationally sensitive neutralizing VP8 MAbs. Three of these

mutants (S114, Y194, and Y219) retained their ability to interact with SA, while the other three (Y155, Y188, and S190) completely lost this capacity. This observation indicates that the VP8 amino acid residues mutated in the latter constructs are essential for the SA-binding activity of the protein, presumably by interacting directly with the SA molecule. In this regard, it is of interest that an RRV neutralization escape variant (selected with MAb 7A12) with a tyrosine-to-phenylalanine change at VP4 amino acid 188 was competent for HA (27), in apparent contrast to our observation that Y188 might be involved in binding to SA. In the case of influenza virus and murine polyomavirus, the binding of tyrosine to SA is proposed to be mediated by its phenolic oxygen (41, 45, 49); thus, the HA activity of the 7A12 variant could be explained by the presence of a tyrosine at position 189, which could form the bond instead of tyrosine 188. An alternate explanation is that tyrosine 189, and not 188, is the one that makes contact with SA. If this is the case, the lack of SA-binding activity of mutant Y188 could be the result of a small structural perturbation caused by the vacated space from the phenoxyl ring of tyrosine. This could cause the side chains of the surrounding amino acids (lysine 187 and tyrosine 189) to compensate for it, thus disturbing the binding site. On the other hand, histidine (in rotavirus SA11 [see below]) and phenylalanine (in the RRV 7A12 escape variant) have bulky side chains, which could fit well in place of the tyrosine phenoxyl ring, leaving the spatial orientation of the neighboring amino acids unaffected.

Of the potential amino acids involved in the interaction with SA, tyrosine 155 is found only in some of the HA-positive rotavirus strains, with histidine being the replacement in the other SA-binding strains (Table 2). On the other hand, tyrosines 188 and 189 and serine 190 are present in all HA-positive strains, with the exception of simian rotavirus SA11, which has a histidine at position 188. Single mutations in any of these three amino acids (188 to 190) abolished binding to SA, but the tyrosine 189 mutation partially affected the structure of the protein, most probably reflecting its relevance for the conformation of VP8.

The only HA-negative rotavirus strain that has tyrosine residues at positions 155, 188, and 189 and serine at position 190 of VP4 is the murine strain EW. However, this protein has a deletion of two amino acids (residues 193 and 194 according to the RRV VP4 numbering), which are in close proximity to the triplet YYS188–190 (Table 2). This deletion might be altering the structure of the EW VP4 SA-binding domain, resulting in its HA-negative phenotype. All the other HA-negative strains analyzed have nonconservative substitutions in at least one (more commonly two) of the residues proposed to be involved in SA binding (Table 2). These observations provide further support for the suggestion that residues 155 and 188 to 190 are essential for SA-binding activity.

Structurally important domains have been localized close to the VP8 triplet YYS188–190. Zhou et al. (53) have suggested that the region around amino acids 180 and 183, described as epitope NP1b, is critical for VP4-VP7 interactions and/or the stability of rotavirus SA11. These authors also found that a change at amino acid 194 (Tyr to Cys) in a virus escape mutant selected with the neutralizing MAb 23 rendered the virus unable to hemagglutinate. In our system, a Tyr-to-Ala change at this amino acid position in GST-VP8 did not modify the HA ability of the protein. This finding suggests that the amino acid change in the SA11 MAb 23 escape mutant altered the local conformation of the protein, particularly of the nearby amino acids Tyr-188, Tyr-189, and Ser-190, resulting in the indirect loss of the virus SA-binding activity. However, it cannot be ruled out that the VP8 amino acids involved in contacting SA vary among rotavirus strains.

TABLE 2. Sequence alignment of the VP4 regions containing the amino acids proposed to be involved in binding to sialic acids

Rotavirus strain	Phenotype[a]	Sequence in[b]: Loop 7	Loop 9
RRV	HA^+	TQNGSYSQ**Y**GPLQSTPKL	NGETPNVTTK--**YYS**TTNYDSVN
SA11	HA^+	TANGSIGQ**Y**GPLLSSPKL	EGQTPNARTA--**HYS**TTNYDSVN
OSU	HA^+	TPTGSYTQ**H**GPLFSTPKL	NGTTPNATTG--**YYS**ATNYDTVN
YM	HA^+	TLTGNYTQ**H**GPLFSTPKL	NGTTPNATTG--**YYS**TTNYDTVN
H1	HA^+	TLTGNYTQ**H**GPLFSTPKL	NGTTPNATTG--**YYS**TTNYDTVN
L338	HA^+	TLDGAYAQ**Y**GPLLSATKL	SGETPNATTA--**YYS**TTNYDTVN
FRV64	HA^+	TQNGSYSQ**Y**GPLLSTPKL	SGQTPNATTG--**YYS**STNYDSVN
Cat97	HA^+	TQNGSYSQ**Y**GPLLSTPKL	SGQTPNATTG--**YYS**ATNYDSVN
Ro1845	HA^+	TQNGSYSQ**Y**GPLLSTPKL	SGQTPNATTG--**YYS**ATNYDSVN
K8	HA^-	TPYGTYTQ**Y**STLSTPHKL	QGATPNASES--**YYL**TINNDNSN
RV5	HA^-	SSQGDFSN**R**RTLTSNNRL	HGETPRATTD--**SSN**TADLNNIS
KU	HA^-	SSQNEFYN**R**RTLTSDTKL	HGETPRATTD--**SSN**TANLNDIS
Wa	HA^-	SSQNEFYN**R**RTLTSDTRF	HGETPRATTD--**SSS**TANLNNIS
1076	HA^-	SVSAEFQH**K**RTLTSDTKL	YGETPHATTD--**YSS**TSNLSEVE
UK	HA^-	AVDGDYAE**W**GTLLSDTKL	EGETPNATTK--**GYF**ITNYASAE
EW	HA^-	PTTGSYVR**Y**NILLSSTKL	VGETPTAGQA--**YYS**SF--NIFN
H2	HA^-	TLSGNFTL**Y**STLLSEPKL	NGETPNATTT--**GYV**TSNYDSLT
69M	HA^-	TSSGTYTQ**H**SPLLSEPKL	NGETPNAITN--**GYP**TTNYDSVN
MDR13	HA^-	SQNDSYTN**Y**GTLLSENKL	TGDTPNAVPYEW**GYT**TNNYDEIV
B223	HA^-	SSTQAYGS**R**NYLNTAHRL	WGADTQGDLRVG**TYS**NPVPNAV-

[a] The HA-positive (HA^+) and HA-negative (HA^-) phenotype of the rotavirus strains is indicated.

[b] The amino acids which are thought to be involved in binding to SA in HA-positive strains and the corresponding amino acids in HA-negative strains are shown in boldface type. The GenBank accession numbers of the rotavirus strains are listed in Materials and Methods.

A panel of murine IgA MAbs directed to the VP8 protein of rotavirus RRV has been recently isolated and characterized (13). One of these MAbs (4B6) selected for a virus escape mutant that failed to hemagglutinate, and the mutated residue was mapped to amino acid residue 190 (Ser to Leu). This observation supports our finding that serine 190 is critical for the binding of the protein to SA. It is of interest that both HA-negative escape mutants (selected with MAbs 23 and 4B6) can grow in cell culture (13, 53). If the site on animal rotavirus VP8 that interacts with SA on the surface of erythrocytes is the same that interacts with the SA-containing cell receptor in MA104 cells, both mutants should not require the initial interaction with SA for infection, in a manner similar to the SA-independent RRV mutants previously described (30).

Méndez et al. (30) recently reported the isolation of RRV mutants with a SA-independent phenotype. The infectivity of these mutants was no longer inhibited by treatment of cells with sialidases or incubation with gphA. Paradoxically, these mutants were still able to hemagglutinate, and this HA was inhibited by gphA. The fact that gphA was able to bind to the mutant viruses but no longer prevented infection suggested that in these mutants there is a second site on the viral surface (independent of the VP8 SA-binding site) which is primarily responsible for interaction with the host cell. A lysine-to-arginine change at position 187 was found to be responsible for the mutant phenotype (31). However, it was not clear whether this amino acid formed part of the SA-independent cell-binding site or whether its change altered the structure of VP4 and exposed the SA-independent binding site located elsewhere in the molecule. The observation that amino acids 188, 189, and

190 might be contacting the SA molecule strongly suggests that the latter possibility is more likely to be correct.

The analysis of the secondary structure of VP8 predicted the presence of 11 β strands separated by loops and flanked by two small α helices. This is in agreement with a previous VP4 secondary-structure prediction obtained by the Garnier and Chou-Fasman algorithms, which described the amino-terminal half of VP4 (which includes VP8) as being rich in β strands (24). A number of variants that escape neutralization by MAbs directed to VP8 have been isolated and characterized for simian rotaviruses RRV and SA11 and human rotavirus ST3, and the amino acid mutations responsible for this phenotype have been mapped (13, 27, 33, 53). Because these amino acid changes allow viruses to escape neutralization, it is thought that they may be part of neutralization epitopes. These epitopes are expected to be exposed on the surface of the protein, most probably in loops. In agreement with this idea, the mutations found in these variants map to loops in the predicted secondary structure of VP8 (Fig. 2). These mutations are distributed in 7 of the 10 loops that separate the 11 β strands. In only three small loops (loop 5, between β strands 5 and 6; loop 8, between β strands 8 and 9; and loop 10, between β strands 10 and 11) have MAb escape mutations not been mapped.

Competition experiments between neutralizing MAbs directed to RRV VP8 (13, 44) have shown that MAb 1A9, which selects for variants with mutations at amino acid 100 (loop 3), competes with MAbs that select for mutations in loop 9: MAbs 7A12 (amino acid 188), 23 (amino acid 194), and 4B6 (amino acid 190). In addition, MAb 1A9 competes with MAbs which select for changes in loop 7: MAbs 5C4 (amino acid 150) and 2B12 (amino acid 148). Also, loop 7 MAb 5C4 competes with loop 9 MAbs 7A12 and 23, and loop 7 MAb 2B12 competes with loop 9 MAb 23. The results obtained from these competitive studies were confirmed through the analysis of the MAb viral antigenic variants in neutralization and HA inhibition assays (13, 44). The antigenic-variant analysis eliminates the steric and diminishes the allosteric potential artifacts present in the competition experiments, although a conformational alteration induced by an amino acid change at a distant site cannot be ruled out. Altogether, these data suggest that loops 3, 7, and 9 are in close proximity, forming a large antigenic domain composed of several distinct epitopes. Indeed, the MAbs that select for amino acid changes in these three loops have been assigned to one of the three serologically defined functional groups (group 3A) described for RRV VP8 (44). The amino acids proposed in this study to form part of the RRV VP8 SA-binding site are located in loops 7 (Tyr-155) and 9 (Tyr-188, Tyr-189, and Ser-190) and therefore would also be predicted to be close to each other. On the other hand, RRV VP8 MAbs that select for changes at amino acids 132 to 135, located in loop 6, have been found not to compete with MAbs that interact with amino acids in loops 3, 7, and 9. In fact, it has been suggested that the epitope from positions 132 to 135 is completely separated from other known antigenic domains of RRV VP4 (13).

The results derived from the MAb competition experiments, the antigenic-variant analysis, and the VP8 secondary-structure prediction and site-directed mutagenesis carried out in this work suggest that VP8 is likely to have an antiparallel β-barrel structure with the odd-numbered loops close to each other and separate from the even-numbered loops. In this regard, it is of interest that rotavirus SA11 VP8 epitopes NP1a and NP1b, defined by amino acids 136 (MAb 9F6) and 180 to 183 (MAbs 7G6 and 10G6), have been described to be in close proximity, as defined by competitive MAb-binding experiments (2). This suggests either that VP8 loops 6 and 9 are closer in SA11 than in RRV or that in SA11 the binding of the first MAb alters the conformation of the protein, allosterically preventing the binding of the second MAb. The latter possibility seems more likely, since analysis of the viral antigenic variants by a plaque reduction neutralization assay identified NP1a and NP1b as separate epitopes (53).

It was recently reported that triple-layered rotavirus SA11 particles disassemble following the binding of NP1b MAbs 7G6 and 10G6 (which select for amino acids 180 and 183, respectively) and this modification of the virion was suggested to be a novel mechanism for rotavirus neutralization (53). Since VP8 seems to bind to SA through a region that is very close to the NP1b epitope, it is tempting to speculate that the binding of the virus to SA on the surface of the target cell could alter the structure of VP4 (and maybe of VP7) and thus help promote the disassembly of the virus outer layer, favoring virus penetration (11). The SA-binding domain of rotavirus VP8 should be highly accessible in the protein, like the SA-binding sites of influenza virus and polyomavirus hemagglutinins, which are located close to the tip of the molecule (45, 49). If this is true, epitope NP1b is more likely to be located in the distal half of VP4, and not close to the base of the spike, near VP7, as has been suggested (53). The interaction of the NP1b MAbs with the virus particle might alter the VP4-VP7 interaction and the virus stability, by a conformational change transmitted from a distant site in the molecule, in a manner similar to that observed for the sigma 1 protein of reovirus when it interacts with SA (7). In fact, analysis of reassortant viruses with surface proteins derived from different parental strains has shown that the reactivity of MAb 2G4, directed to an epitope localized to the distal part of VP4 (36), is influenced by the interaction of VP4 with VP7 (3).

Alanine has been widely used as the substituting amino acid in site-directed mutagenesis studies for its property of not altering the structure of the mutated proteins (5, 14, 15). Despite this, we found that 9 of the 15 mutations tested altered the structure of the protein. Of interest, the amino acids whose mutations lead to severe distortion of the protein structure (Y119, N132, Y152, Y177, and Y206) are conserved in most rotavirus VP4 proteins compared, regardless of their SA-binding phenotype. This observation supports their role in preserving the structure of the protein. The three other amino acids whose change caused a mild distortion of the protein are less highly conserved, but they also probably form part of important structural elements of VP4.

The data obtained in this work concerning the relevance of specific VP8 amino acids for the structure and SA-binding activity of RRV VP8, together with the proposed organization of the secondary structure of this VP4 domain, should help in designing experiments to advance the characterization of the various functional domains of the protein, and they should also support the interpretation of the three-dimensional crystal structure of VP4 when it becomes available.

ACKNOWLEDGMENTS

We thank H. B. Greenberg for kindly providing the MAbs used in this work.

This work was partially supported by grants 75197-527106 from the Howard Hughes Medical Institute, G0012-N9607 from the National Council for Science and Technology—Mexico, IN207496 from DGAPA-UNAM, and ERB3514PL950019 from the INCO Programme of the European Community.

REFERENCES

1. **Anthony, I. D., S. Bullivant, S. Dayal, A. R. Bellamy, and J. A. Berriman.** 1991. Rotavirus spike structure and polypeptide composition. J. Virol. **65:** 4334–4340.

2. **Burns, J. W., H. B. Greenberg, R. D. Shaw, and M. K. Estes.** 1988. Functional and topographical analyses of epitopes on the hemagglutinin (VP4) of the simian rotavirus SA11. J. Virol. **62:**2164–2172.
3. **Chen, D. Y., M. K. Estes, and R. F. Ramig.** 1992. Specific interactions between rotavirus outer capsid proteins VP4 and VP7 determine expression of a cross-reactive, neutralizing VP4-specific epitope. J. Virol. **66:**432–439.
4. **Crawford, S., M. Labbé, J. Cohen, M. H. Burroughs, Y.-J. Zhou, and M. K. Estes.** 1994. Characterization of virus-like particles produced by the expression of rotavirus capsid proteins in insect cells. J. Virol. **68:**5945–5952.
5. **Cunningham, B. C., and J. A. Wells.** 1989. High-resolution epitope mapping of hGH-receptor interactions by alanine-scanning mutagenesis. Science **244:** 1081–1085.
6. **Estes, M. K., and J. Cohen.** 1989. Rotavirus gene structure and function. Microbiol. Rev. **53:**410–449.
7. **Fernandes, J., D. Tang, G. Leone, and P. W. K. Lee.** 1994. Binding of reovirus to receptor leads to conformational changes in viral capsid proteins that are reversible upon virus detachment. J. Biol. Chem. **269:**17043–17047.
8. **Fiore, L., H. B. Greenberg, and E. R. Mackow.** 1991. The VP8 fragment of VP4 is the rhesus rotavirus hemagglutinin. Virology **181:**553–563.
9. **Fuentes-Pananá, E. M., S. López, M. Gorziglia, and C. F. Arias.** 1995. Mapping the hemagglutination domain of rotaviruses. J. Virol. **69:**2629–2632.
10. **Fukudome, K., O. Yoshie, and T. Konno.** 1989. Comparison of human, simian, and bovine rotaviruses for requirement of sialic acid in hemagglutination and cell adsorption. Virology **172:**196–205.
11. **Fukuhara, N., O. Yoshie, S. Kitaoka, and T. Konno.** 1988. Role of VP3 in human rotavirus internalization after target cell attachment via VP7. J. Virol. **62:**2209–2218.
12. **Geourjon, C., and G. Deleage.** 1994. SOPM: a self optimised prediction method for protein secondary structure prediction. Protein Eng. **7:**157–164.
13. **Giammarioli, A. M., E. R. Mackow, L. Fiore, H. B. Greenberg, and F. M. Ruggeri.** 1996. Production and characterization of murine IgA monoclonal antibodies to the surface antigens of rhesus rotavirus. Virology **225:**97–110.
14. **Gibbs, C. S., and M. J. Zoller.** 1991. Rational scanning mutagenesis of a protein kinase identifies functional regions involved in catalysis and substrate interactions. J. Biol. Chem. **266:**8923–8931.
15. **Grodberg, J., K. L. Davis, and A. J. Sytkowski.** 1993. Alanine scanning mutagenesis of human erythropoietin identifies four amino acids which are critical for biological activity. Eur. J. Biochem. **218:**597–601.
16. **Kaljot, K. T., R. D. Shaw, D. H. Rubin, and H. B. Greenberg.** 1988. Infectious rotavirus enters cells by direct cell membrane penetration, not by endocytosis. J. Virol. **62:**1136–1144.
17. **Kapikian, A. Z., and R. M. Chanock.** 1996. Rotaviruses, p. 1657–1708. *In* B. N. Fields, D. M. Knipe, and P. M. Howley (ed.), Fields virology, vol. 2. Lippincott-Raven, Philadelphia, Pa.
18. **Keljo, D. J., and A. K. Smith.** 1988. Characterization of binding of simian rotavirus SA-11 to cultured epithelial cells. J. Pediatr. Gastroenterol. Nutr. **7:**249–256.
19. **Laemmli, U. K.** 1970. Cleavage of structural proteins during the assembly of the head of bacteriophage T4. Nature **227:**680–685.
20. **Lim, K., J. X. Ho, K. Keeling, G. L. Gilliland, X. Ji, F. Ruker, and D. C. Carter.** 1994. Three-dimensional structure of Schistosoma japonicum glutathione S-transferase fused with a six-amino acid conserved neutralizing epitope of gp41 from HIV. Protein Sci. **3:**2233–2244.
21. **Lizano, M., S. López, and C. F. Arias.** 1991. The amino-terminal half of rotavirus SA114fM VP4 protein contains a hemagglutination domain and primes for neutralizing antibodies to the virus. J. Virol. **65:**1383–1391.
22. **López, S., and C. F. Arias.** 1993. Protein NS26 is highly conserved among porcine rotavirus strains. Nucleic Acids Res. **21:**1042.
23. **López, S., R. Espinosa, H. B. Greenberg, and C. F. Arias.** 1994. Mapping the subgroup epitopes of rotavirus protein VP6. Virology **204:**153–162.
24. **López, S., I. López, P. Romero, E. Méndez, X. Soberón, and C. F. Arias.** 1991. Rotavirus YM gene 4: analysis of its deduced amino acid sequence and prediction of the secondary structure of the VP4 protein. J. Virol. **65:**3738–3745.
25. **Ludert, J. E., N. Feng, J. H. Yu, R. L. Broome, Y. Hoshino, and H. B. Greenberg.** 1996. Genetic mapping indicates that VP4 is the rotavirus cell attachment protein in vitro and in vivo. J. Virol. **70:**487–493.
26. **Mackow, E. R., J. W. Barnett, H. Chan, and H. B. Greenberg.** 1989. The rhesus rotavirus outer capsid protein VP4 functions as a hemagglutinin and is antigenically conserved when expressed by a baculovirus recombinant. J. Virol. **63:**1661–1668.
27. **Mackow, E. R., R. D. Shaw, S. M. Matsui, P. T. Vo, M. N. Dang, and H. B. Greenberg.** 1988. The rhesus rotavirus gene encoding protein VP3: location of amino acids involved in homologous and heterologous rotavirus neutralization and identification of a putative fusion region. Proc. Natl. Acad. Sci. USA **85:**645–649.
28. **Mackow, E. R., M. Y. Yamanaka, M. N. Dang, and H. B. Greenberg.** 1990. DNA amplification-restricted transcription-translation: rapid analysis of rhesus rotavirus neutralization sites. Proc. Natl. Acad. Sci. USA **87:**518–522.
29. **Markwell, M. A. K., L. Svennerholm, and J. C. Paulson.** 1981. Specific gangliosides function as host cell receptor for Sendai virus. Proc. Natl. Acad. Sci. USA **78:**5406–5410.
30. **Méndez, E., C. F. Arias, and S. López.** 1993. Binding to sialic acids is not an essential step for the entry of animal rotaviruses to epithelial cells in culture. J. Virol. **67:**5253–5259.
31. **Méndez, E., C. F. Arias, and S. López.** 1996. Interactions between the two surface proteins of rotavirus may alter the receptor-binding specificity of the virus. J. Virol. **70:**1218–1222.
32. **Merino, E., J. Osuna, F. Bolívar, and X. Soberón.** 1992. A general PCR-based method for single or combinatorial oligonucleotide-directed mutagenesis on pUC/M13 vectors. BioTechniques **12:**508–510.
33. **Padilla, N. L., S. J. Dunn, S. López, H. B. Greenberg, and C. F. Arias.** 1995. Identification of two independent neutralization domains on the VP4 trypsin cleavage products VP5* and VP8* of human rotavirus ST3. Virology **206:** 148–154.
34. **Patton, J. T., J. Hua, and E. A. Mansell.** 1993. Location of intrachain disulfide bonds in the VP5* and VP8* trypsin cleavage fragments of the rhesus rotavirus spike protein VP4. J. Virol. **67:**4848–4855.
35. **Paul, R. W., A. H. Choi, and P. W. Lee.** 1989. The alfa-anomeric form of sialic acid is the minimal receptor determinant recognized by reovirus. Virology **159:**94–101.
36. **Prasad, B. V., J. W. Burns, E. Marietta, M. K. Estes, and W. Chiu.** 1990. Localization of VP4 neutralization sites in rotavirus by three-dimensional cryo-electron microscopy. Nature **343:**476–479.
37. **Rose, G. D., A. R. Geselowitz, G. J. Lesser, R. H. Lee, and M. H. Zehfus.** 1985. Hydrophobicity of amino acid residues in globular proteins. Science **229:**834–838.
38. **Rost, B., and C. Sander.** 1994. Combining evolutionary information and neural networks to predict protein secondary structure. Proteins **19:**55–72.
39. **Rost, B., and C. Sander.** 1994. Conservation and prediction of solvent accessibility in protein families. Proteins **20:**216–226.
40. **Rost, B., and A. Valencia.** 1996. Pitfalls of protein sequence analysis—commentary. Curr. Opin. Biotechnol. **7:**457–461.
41. **Sauter, N. K., J. P. Hanson, G. D. Glick, J. H. Brown, R. L. Crowther, S.-J. Park, J. J. Shekel, and D. C. Wiley.** 1992. Binding of influenza virus hemagglutinin to analogs of its cell-surface receptor, sialic acid: analysis by proton nuclear magnetic resonance spectroscopy and X-ray crystallography. Biochemistry **31:**9609–9621.
42. **Schendel, P. F.** 1994. Expression and purification of glutathione-S-transferase fusion proteins, p. 16.7.1–16.7.7. *In* F. M. Ausubel, R. Brent, R. E. Kingston, D. D. Moore, J. G. Seidman, J. A. Smith, and K. Struhl (ed.), Current protocols in molecular biology. John Wiley & Sons, Inc., New York, N.Y.
43. **Shaw, A. L., R. Rothnagel, D. Chen, R. F. Ramig, W. Chiu, and B. V. Prasad.** 1993. Three-dimensional visualization of the rotavirus hemagglutinin structure. Cell **74:**693–701.
44. **Shaw, R. D., P. T. Vo, P. A. Offit, B. S. Coulson, and H. B. Greenberg.** 1986. Antigenic mapping of the surface proteins of rhesus rotavirus. Virology **155:**434–451.
45. **Stehle, T., Y. Yan, T. L. Benjamin, and S. C. Harrison.** 1994. Structure of murine polyomavirus complexed with an oligosaccharide receptor fragment. Nature **369:**160–163.
46. **Stultz, C. M., J. V. White, and T. F. Smith.** 1993. Structural analysis based on state-space modeling. Protein Sci. **2:**305–314.
47. **Taniguchi, K., T. Urasawa, and S. Urasawa.** 1994. Species specificity and interspecies relatedness in VP4 genotypes demonstrated by VP4 sequence analysis of equine, feline, and canine rotavirus strains. Virology **200:**390–400.
48. **Vlasak, R., W. Luytjes, W. Spaan, and P. Palese.** 1988. Human and bovine coronaviruses recognize sialic acid-containing receptors similar to those of influenza C viruses. Proc. Natl. Acad. Sci. USA **85:**4526–4529.
49. **Weis, W., J. H. Brown, S. Cusack, J. C. Paulson, J. J. Skehel, and D. C. Wiley.** 1988. Structure of the influenza virus haemagglutinin complexed with its receptor, sialic acid. Nature **333:**426–431.
50. **White, J. V., C. M. Stultz, and T. F. Smith.** 1994. Protein classification by stochastic modeling and optimal filtering of amino-acid sequences. Math. Biosci. **119:**35–75.
51. **Williams, W. V., T. Kieber-Emmons, D. B. Weiner, D. H. Rubin, and M. I. Greene.** 1991. Contact residues and predicted structure of the reovirus type-3 receptor interaction. J. Biol. Chem. **266:**9241–9250.
52. **Yolken, R. H., R. Willoughby, S. B. Wee, R. Miskuff, and S. Vonderfecht.** 1987. Sialic acid glycoproteins inhibit in vitro and in vivo replication of rotaviruses. J. Clin. Invest. **79:**148–154.
53. **Zhou, Y. J., J. W. Burns, Y. Morita, T. Tanaka, and M. K. Estes.** 1994. Localization of rotavirus VP4 neutralization epitopes involved in antibody-induced conformational changes of virus structure. J. Virol. **68:**3955–3964.